THE STRENGTH AND DYNAMIC ANALYSIS OF THE PROTOTYPE OF TESLA TURBINE

Paweł BAGIŃSKI[1], Łukasz JĘDRZEJEWSKI[2]

THE SZEWALSKI INSTITUTE OF FLUID-FLOW MACHINERY
POLISH ACADEMY OF SCIENCES.
[1]TURBINE DYNAMICS AND DIAGNOSTICS DEPARTMENT
[2]TURBINE DEPARTMENT
FISZERA 14, 80-231 GDANSK, POLAND
E-mail: pbaginski@imp.gda.pl
Work phone: (48 58) 69 95 274

Summary

This article presents the strength and modal analysis of the rotor model of the Tesla micro-turbine. The calculations were made in order to verify the design of multi-disc turbine's rotor before production process. Two commercial solvers were used independently, which are capable to deal with problems of solid state physics – Abaqus and Ansys Mechanical with Workbench software. The comparison of results from two applications aimed at checking solvers' applicability in the present case. Preliminary analysis was carried out in Abaqus software. The calculations were performed assuming perfect bearing stiffness for different rotation speeds. A more detailed analysis was made in Ansys Mechanical software using structure analysis modules to determine the stresses in the structure which arise as a consequence of rotor's rotational motion. Subsequently, it was followed up with modal analysis results. Additionally the parameters of selected bearings were determined and modal analysis took into account the stiffness corresponding to individual rolling bearings.

Keywords: turbine dynamics, strength, Tesla turbine, modal analysis

BADANIA WYTRZYMAŁOŚCIOWE I DYNAMICZNE PROTOTYPU TURBINY TESLI

Streszczenie

W niniejszej artykule przedstawiono wyniki analizy wytrzymałościowej i dynamicznej prototypu modelu wirnika mikroturbiny Tesli. Analizy zostały przeprowadzone w celu sprawdzenia i weryfikacji projektu wielodyskowego wirnika turbiny Tesli przed etapem produkcyjnym. Obliczenia zostały przeprowadzone niezależnie przy pomocy dwóch komercyjnych solwerów do analizy mechaniki ciała stałego - Abaqus oraz Ansys Mechanical w środowisku Workbench. Porównanie wyników z dwóch aplikacji ma na celu wzajemną weryfikację stosowalności solwerów do omawianego przypadku. Wstępna analiza została wykonana w programie Abaqus. Obliczenia zostały wykonane przy założeniu całkowitej sztywności łożysk i zadanej prędkości obrotowej. Dokładna analiza została wykonana w programie Ansys Mechanical w środowisku Workbench przy wykorzystaniu modułów do analizy strukturalnej w celu wyznaczenia wstępnego stanu naprężeń będącego konsekwencją ruchu obrotowego wirnika oraz modułu analizy modalnej. Dodatkowo wyznaczono parametry wstępnie dobranych łożysk i wykonano analizę modalną uwzględniającą sztywności właściwe dla zastosowanych typów poszczególnych łożysk tocznych.

Słowa kluczowe: Dynamika turbin, wytrzymałość, turbina Tesli, analiza modalna

1. PREFACE

The Tesla turbine was patented by Serbian inventor Nikola Tesla in 1913 (1). It is referred to as a bladeless turbine (Fig. 1). The rotor's turning motion is provided by boundary layer effect and adhesion. Tesla's design sidestepped the key drawbacks of the bladed turbines but it does suffer from the problem of flow restrictions. The total number of thin rotor disks varies from several to tens(the number of disks increases as higher flow rate is required). The disks are fixed directly to the shaft in a direction perpendicular to its axis of rotation. The article (2) shows that you can get the biggest improvements in efficiency when the disks

are as thin as possible and the distances between them are as minimal as possible.

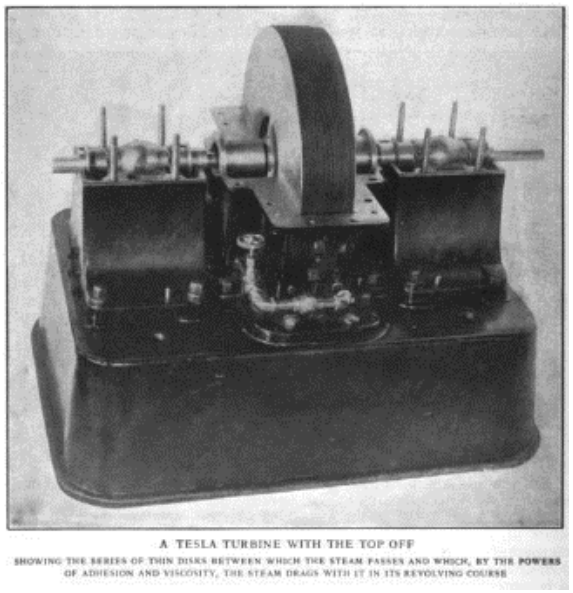

Fig. 1. The Tesla turbine, in accordance with patent documentation (1)

The distance between the adjacent disks is strictly dependent on existing flow parameters and the type of working medium used. These values are evidently limited by mechanical properties of the material from which the rotor is made as well as by manufacturing and assembly processes. Figure 2 shows an example of a design of multiple-disk rotor in a Tesla turbine, in accordance with patent documentation (3). The power supply of the turbine can be established in two ways. The first option is to use nozzles that are evenly mounted along the circumference of the shaft, at a precisely adjusted angle against the plane tangential to the external outline of the disk. Option 2 assumes that the outlet area is simplified in a way that the medium can flow out from the turbine's flow passage along the entire circumference of the shaft, in a radial direction. Similar solution may be found in centrifugal pumps which have main channel on the outer edge. Application of such a solution requires installation of additional steering in the main channel which directs the working medium into spaces between disks at a right angle. The spiral movements of the working medium from the inlet to the exhaust undergo many rotations. When the load increases the number of rotations drops and the spiral taken by the fluid becomes progressively shorter.

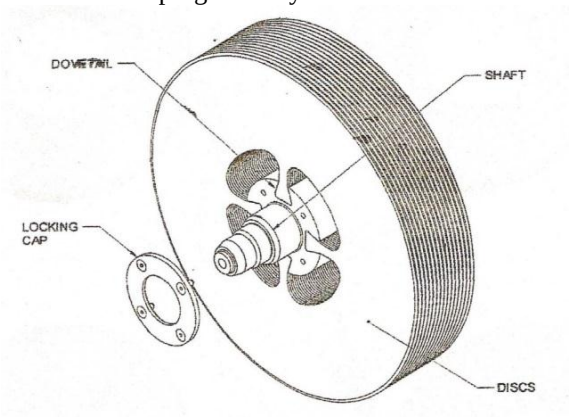

Fig. 2. Multiple-disk rotor in a Tesla turbine (3)

Outflow of the working medium from the disk interspaces takes place in the axial direction through a number of holes in the disks located near to turbine shaft. Such a solution for outflow was proposed by Nikola Tesla in his patent documentation (1) and subsequent patent documentations presented by Keneth Hicks (3). Fig. 3 demonstrates schematically the Tesla turbine as well as the flow direction of the working medium.

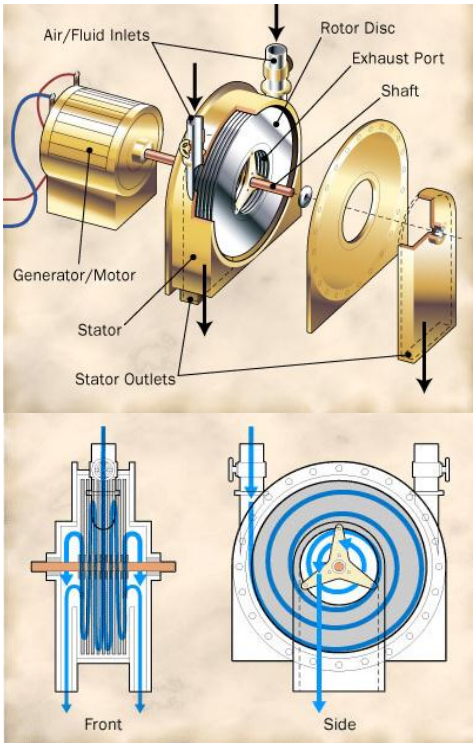

Fig. 3. Diagram of example design of Tesla turbine (a), flow direction of the working medium between turbine disks(b)

Due to the construction of the rotor (consisting of many thin disks), its mode of action and high-speed

operations of the order of several dozen thousand rpm and even higher, bladeless rotor of the turbine is exposed to significant impact of stresses generated by centrifugal force. Method of affixing of the disks on the shaft or close to centrally located outlet holes and lack of mounting points on the external perimeter may cause additional difficulties linked to the relatively low structure rigidity of the whole rotor. The authors are of the opinion that doing an appropriate dynamic mechanical analysis was necessary. The aim of the analysis was to calculate the first few natural frequencies of the rotor and determination of rotational speed interval for which the operations is safe.

2. NUMERICAL MODEL GEOMETRY OF THE TESLA TURBINE

The original construction, according to the patent of Nikola Tesla, assumes that the disks are mounted directly on the shaft and blocking them by a cover and a turnbuckle (fig. 2). Such an assembly forces that the outflow of the working medium from the disk interspaces takes place through the holes situated in the disks. During turbine operation outlet holes change its position in relation to supply nozzles being a source of non-stationary flow in the turbine's rotor. Disk fixation method on the shaft is also important for the structure rigidity of the rotor. In the classic construction the location of disk blocking is close to the shaft, with a relatively small radius, which in the case of disks with larger cross-sections results in a sharp drop in rigidity. That, in combination with non-stationary flow inside the rotor may lead to the occurrence of unwanted dynamic effects and to elevated vibration level at high rotor speeds. The situation where the outflow of the working medium in radial direction is unhindered appears to be the most favorable. It is not achievable in real time model due to construction reasons. The disks must be connected to the shaft for better transfer of the torque generated on their surface. The working medium outflow in the radial direction can be realized through an alternative solution for disk fixation which is to connect them by means of bars (Fig.4). Such a construction allows making considerably thinner shaft at the point of outflow. The disks fixing point is situated further from the axis of rotation, improving rigidity of the structure. This construction solution brings an obstacle into the flow channel in the form of a bar and a spacer what, as in the case of classic construction, may result in the occurrence of non-stationary flow. Such interaction cannot be totally eliminated. Additionally, during the outflow from the disk interspaces a change in flow direction must occur, from spiral – in a plane perpendicular to the axis of rotation to axial. This change may proceed with varying intensity, more or less aggressively, making it necessary to increase the flow workspace where the change takes place.

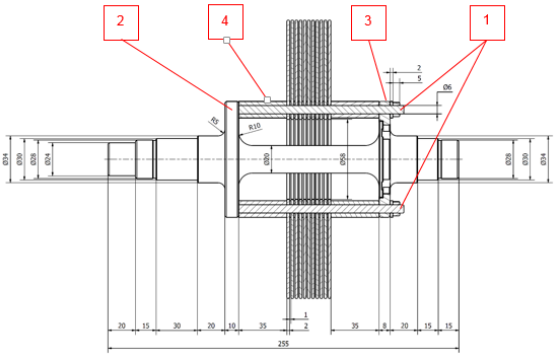

Fig. 4. The alternative concept for the rotor of Tesla turbine. 1 – binding bars, 2 – solid disk manufactured as an integral part of the shaft, 3 – removable disk, locked on the shaft by a hollow joint, 4 – spacing sleeves

Four bars binding the multiple-disk rotor, distributed evenly over the circumference, are presented on Fig. 4 (no. 1). They are blocked by disks, with one (no. 2) being an integral part of the shaft and the disk no. 3 fixed to it by a hollow joint. Between the group of thin disks and the other two disks the spacing sleeves were situated (no. 4). As a result, the disks no. 2 and no. 3 are within a certain distance from rotating disks, thereby creating a flow channel, allowing the free outflow of the working medium from the thin disks interspace along the entire perimeter. The following assumptions were applied to the model, which are the consequence of the flow calculations already carried out (4).

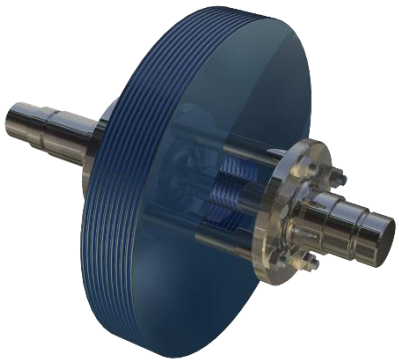

Fig. 5. 3D model of multiple-disk rotor of the Tesla turbine

The number of thin disks was equal to 11. Thickness of every disk was identical – 2mm and the value of disk interspace was set to 1mm. This distance was obtained using spacing sleeves which are fitted onto all four bars. 3D visualization of the rotor was shown on Fig.5.

2.1 Calculation model in Abaqus software

A quarter of the size of turbine was modelled and then the calculations were performed using so-called cyclosymmetry (Fig. 6).

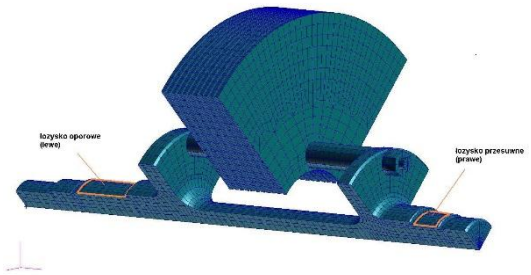

Fig. 6. The Tesla turbine FEA mesh – a quarter of the size of turbine was modelled

Table 1 shows mesh parameters that were used for calculations in Abaqus. Material properties were as follows: density 7850 kg/m3, Young's modulus 2.05E+11, Poisson ratio 0.3.

Table 1 Mesh parameters used for Abaqus calculations

	Model
Number of elements	21592
Number of nodes	105813
Total number of variables in the model	634878
Model mass [kg]	**7.093142**
Moment of inertia IXX [kgmm^2]	28134.57
Moment of inertia IYY [kgmm^2]	168585
Moment of inertia IZZ [kgmm^2]	168585

2.2 Calculation model in Ansys software

The turbine model was discretized in a finite-dimensional space using mesh preprocessor named GAMBIT 2.4.6. The model was split into many blocks, in order to generate heksahedral mesh over its entire volume. This split was done in GAMBIT software and the number of solid bodies – mesh blocks amounted to 310. This large number of blocks is due to the optimization of the solid bodies division into blocks in order to get the best quality of the mesh, and also due to model complexity which consists of many elements such as disks, washers and spacing sleeves. The total number of finite elements in the mesh was equal to 405 320 and the number of nodes 468 587. The transformation of the mesh, prepared in external mesh generator, takes place in Finite Element Modeller application. This tool allows the generation of proper models for strength calculations on the basis of only 3D mesh. The mesh transformation process in the Finite Element Modeller software is shown on Fig. 7. Moreover, it is possible to define contact surfaces for a multi solid body model.

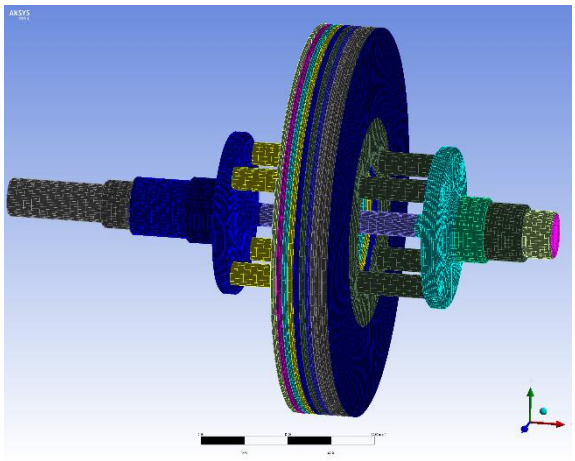

Fig. 7. Dense mesh of the rotor model of the Tesla turbine

On the basis of assumed rotational speed rolling bearings of the Japanese producer NSK were pre-selected. For the support fixed in position, carrying axial load, angular contact O matched pair ball bearings for high accuracy of arrangement, standard series - no. **7906C** was chosen. For the sliding support double-row roller bearing was chosen, increased stiffness series (series no. 30) - **NN3006TBKR**. Rolling bearing stiffnesses of the Tesla turbine were determined on the basis of dependencies in the book (5) and in the catalogue (6). These dependencies were based on the Hertz theory and verified experimentally. Below is presented how the bearing stiffnesses were calculated:

double-row roller bearing (increased stiffness series) - NN3006TBKR

The nominal mutual displacement of the bearing rings is calculated in following way:

$$\delta_r = \frac{5{,}2\, l^{0{,}1}}{\cos\alpha}\left(\frac{F_r D}{C_0}\right)^{0{,}9} \quad (1)$$

$$\delta_r = 0{,}19\ \mu m \quad (2)$$

Nominal bearing stiffness amounts to:

$$c_r = 3{,}45 i Z \cos\alpha^{2{,}1}\ l^{0{,}9}\ \delta_r^{0{,}33} \quad (3)$$

$$c_r = 5{,}23 \times 10^8\ \frac{N}{m} \quad (4)$$

Double-purpose ball bearing 7906C (O matched pair of bearings) where the stiffness value was taken from the catalogue (6).

Pretension force:

$$F_n = 24\ N \quad (5)$$

Stiffness in the axial direction:

$$c_a = 2{,}5 \times 10^7\ \frac{N}{m} \quad (6)$$

Stiffness in the radial direction:

$$c_r = 6{,}5\ \delta_a = 1{,}63 \times 10^8\ \frac{N}{m} \quad (7)$$

The rolling bearing stiffness values showed in Table 2 were selected for further analysis. In the case of O matched double-purpose pair of bearings (**7906C**)

,operating in parallel, substitute stiffness of two bearings in radial direction is the sum of their stiffnesses. In the axial direction this is not the case, as each bearing transfers the forces in the opposite sense.

Table 2. Stiffness coefficients of the rolling bearings used for the rotor dynamics analysis.

Bearing designation	**NN3006TBKR [N/m]**	**7906C [N/m]**
Radial stiffness	5.23×10^8	$2 \times 1.63 \times 10^8$
Axial stiffness	-	2.5×10^7

3. CALCULATION RESULTS OF THE TESLA TURBINE

The Tesla turbine calculations were carried out in ABAQUS and ANSYS software. Disks were fixed to a shaft using bars passing through thin disks and bolted to the thick disks that are attached to a shaft (Fig. 5).

3.1 Calculation results from Abaqus

After modal analysis of Tesla turbine rotor using the arrangement described above it can be observed that the frequencies of free vibrations are higher than 300 Hz and this means that there is no resonance throughout the start-up range up to the nominal speed.

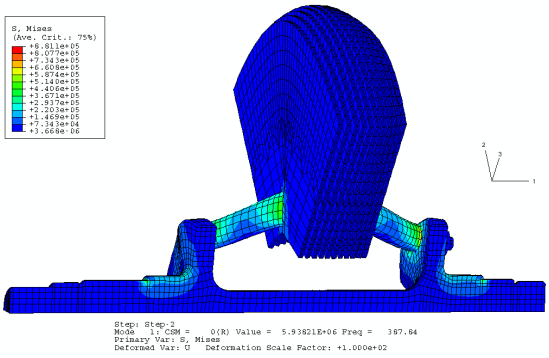

Fig. 8. Deflections and stress distribution for the first mode shape, f=387.84 [Hz], rotational speed = 18000 rpm

Some sample mode shapes are described below. All visualizations present vibrations without averages at nodal points and in deflection scale multiplied by 100. The first mode shape (Fig. 8) indicates that disk vibrations in a plane perpendicular to rotor's axis was due to the speed and occurred at 387.84 [Hz].
The second mode shape (Fig. 9) occurred at 476.64 [Hz] and illustrates the displacements of all disks in the axis direction. The rotor remained stable. The next frequency of free vibrations (Fig. 10) occurred at 483.15 [Hz], that was disks vibrations only where external disks vibrated in the opposite direction towards each other and had the highest vibration amplitude.

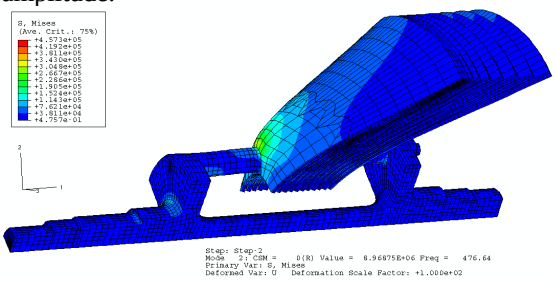

Fig. 9. Deflections and stress distribution for the second mode shape, f=476.64 [Hz], rotational speed = 18000 rpm

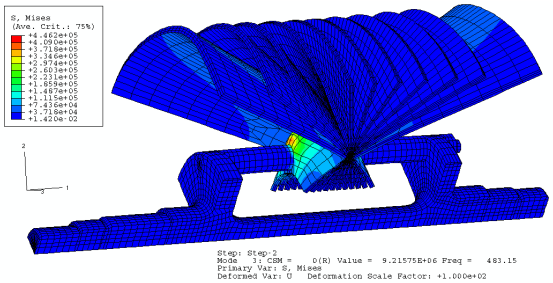

Fig. 10. Deflections and stress distribution for the third mode shape, f=483.15 [Hz], rotational speed = 18000 rpm

The next mode shape was presented using three quarters of the size of turbine's rotor (Fig. 11). Disks vibrations could be observed.

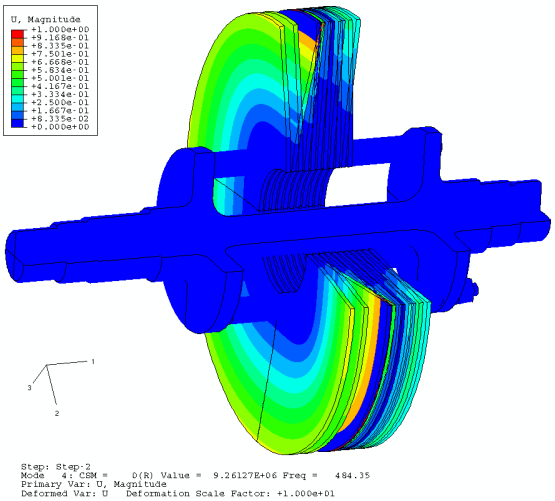

Fig. 11. Deflections for the fourth mode shape, f=484.35 [Hz]. rotational speed = 18000 rpm. (Deflection scale multiplied by 10)

This mode shape and the following ones illustrate disks displacements in different configurations. The shaft was rigid enough to prevent distortion and vibration. Table 3 presents frequency values which were obtained during the rotor dynamics analysis.

The table compares three options: a - the rotor at rest, b - the rotor rotates with bearings having ideal stiffness, c - like in b but with given stiffness of bearings.

Table 3 Frequency values obtained from the Tesla turbine calculations

No.	without rotations [Hz]	Bearings with ideal stiffness [Hz]	Given stiffness of bearings [Hz]
1	361.96	387.84	0
2	361.96	476.64	267,25
3	365.01	483.15	470,63
4	365.01	484.35	471,73
5	371.36	484.37	471,76
6	371.36	484.63	472,07
7	371.54	484.77	472,25
8	371.54	484.78	472,37
9	371.61	485.07	472,53
10	371.61	485.16	472,72

The highest values of reduced stress occurred on the lower edge of the disks and were around 261 MPa (Fig. 12, 13). High values of stress could also be noticed around the connection places of the shaft and binding bars and amounted to 240 MPa (Fig. 14).

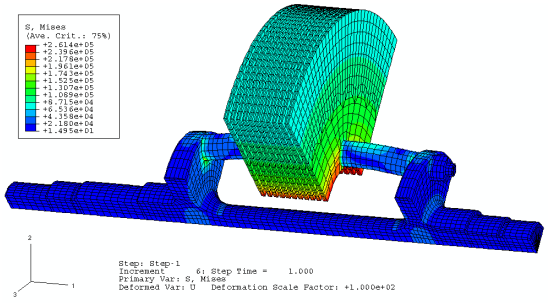

Fig. 12. Equivalent stress (Von Mises) distribution, Smax=261MPa

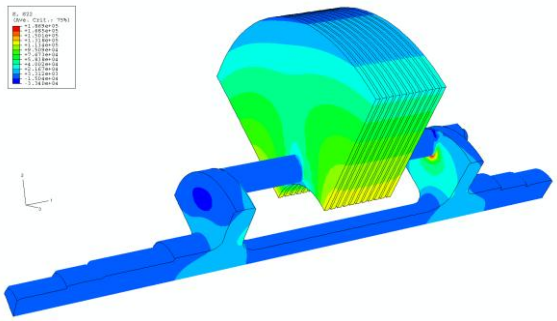

Fig. 13. Normal stress distribution S22, S22max=187MPa

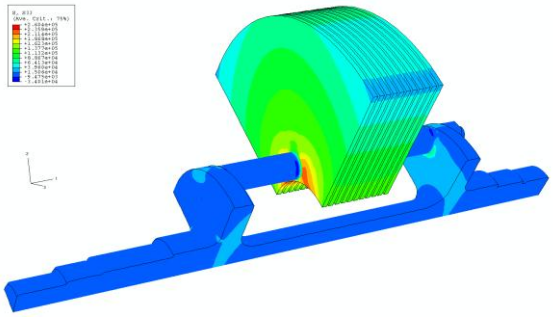

Fig. 14. Normal stress distribution S33, S33max=260MPa

3.2 Calculation results from Ansys

Once the rotor was calculated, the mode shapes and the corresponding frequencies were received. It can be concluded that the results of modal analysis are significantly affected by the values of bearing stiffness. The results in the case of calculated stiffness are radically different from those with ideal stiffness.

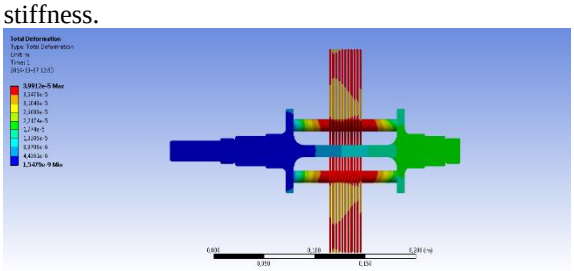

Fig. 15. Deformations caused by given rotary movements

Fig. 15 shows the deformation analysis results where the rotor was supported by rolling bearings at the speed of 18000 rpm. As expected, the greatest amount of deflection (4 μm) occurred at midpoint of the shaft. Such data were used as input data for further analysis.

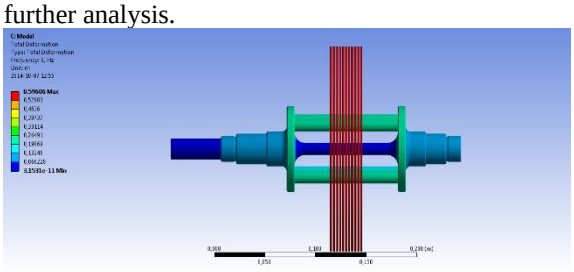

Fig. 16. First mode shape, occurring at around 0 Hz

The first mode shape occurred at the frequency around 0 Hz. Rotor's rotational vibration was the source of these rigid body vibrations. In the case of rigid bearings this mode shape does not appear. This mode is unimportant for longer machine life as well as for safety reasons.

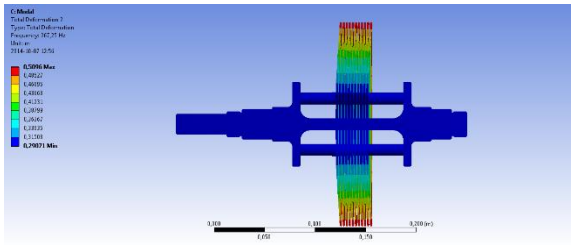

Fig.17. The second mode shape, occurring at 267 Hz

The next mode shape occurring at the frequency of 267 Hz presented vibrations of the entire rotor in the axial direction. The disks were following the shaft and after momentary stiffness increase in double-purpose bearing they deflected. It seems that the double-purpose bearings will be properly transferring the forces stemming from this vibration. In the analysis with rigid bearings this mode shape does not occur. The conclusion can thus be drawn that the first two resonant vibrations of the entire rotor depend on the stiffness of the bearings. Further obtained modes concern disks attached to the shaft.

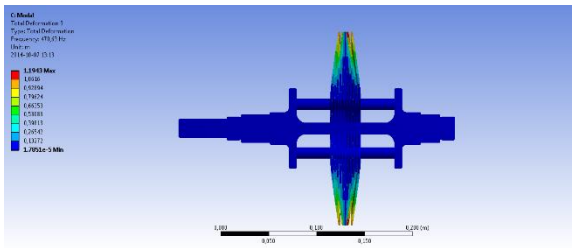

Fig. 18. Third mode shape, 470 Hz

The third mode shape occurred at the frequency of 470 Hz. During these vibrations the disks get close to each other and drift apart from each other in a repeat pattern. As far as this turbine is concerned, where the distances between disks are very short and should be constant, this mode shape is undesirable. The fourth mode shape once again concerned the disks and occurred at the frequency of 471.71 Hz (Fig. 19). Consecutive mode shapes relate to disks which vibrate in a different order and can be distinguished by their shape.

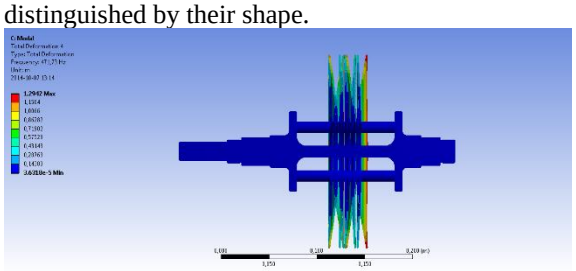

Fig. 19. Fourth mode shape, occurring at 471.71 Hz

In the next parts of this article, the impact of rolling bearing parameters on the frequency values of the mode shapes is discussed. The value of stiffness was changed manually several times in all bearings before repeating the modal analysis calculations. The relation between various given stiffnesses and obtained frequency values for the first three mode shapes is presented on Fig. 20. The value '1' occurs always on the diagonal, as this is autocorrelation.

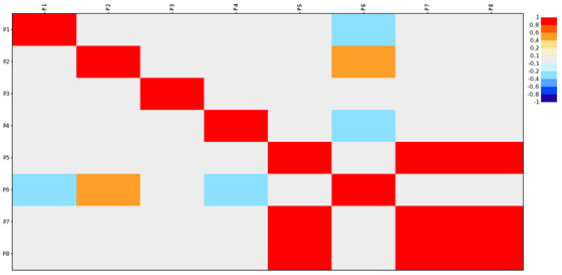

Fig. 20. Correlation between the bearing stiffness and obtained mode shapes

It can be noted that the parameters P1, P2, P4 affect P6 parameter (the first mode shape). The parameters P1, P2, P4 are: roller bearing stiffness in the X direction, roller bearing stiffness in the Y direction, double-purpose bearing stiffness in the Y direction. The second and the third mode shape is affected by the value of the double-purpose bearing stiffness in the axial direction. It follows that control of bearing stiffness allows us to get desirable mode shapes.

4. CONCLUSIONS DRAWN FROM THE CALCULATION RESULTS

Abaqus analysis showed that all frequencies of mode shapes, for all calculation cases, are larger than 300 Hz (which corresponds to 18000 rpm). This means that there is no resonance throughout the start-up range up to the nominal speed. The highest values of reduced von Mises stresses occurred on the lower edge of the disks, at points between binding bars, and were equal to 261 MPa. High values of stress were also noticed at points where the binding bars connect to the disks attached to the shaft (at the bottom, on the internal side) and amounted to 240 MPa.

The modal analysis calculations in Ansys with precalculated bearing stiffness resulted in a decrease of the values of the mode shape frequencies. One of the mode shapes, occurring at 267.25 Hz can influence on the turbine's rotor operation as nominal speed is 300 Hz. That can be no assurance that the stiffnesses listed in the catalogue and also the calculated ones were correct. It was therefore decided to test the impact of the value of stiffness on the frequencies of mode shapes. This way, it can be checked if the change of the stiffness value in any bearing can result in obtaining any frequency value corresponding to any mode shape close to 300 Hz. As can be seen on above figures, the double-purpose bearing stiffness in the axial direction has the greatest influence on obtained frequencies. Besides that, the double-purpose bearing stiffness in the radial direction is a parameter which influences third mode shape and the resulting frequency is close to the nominal frequency. According to the

catalogue the value of both these stiffnesses is equal to 3,25e8 N/m.

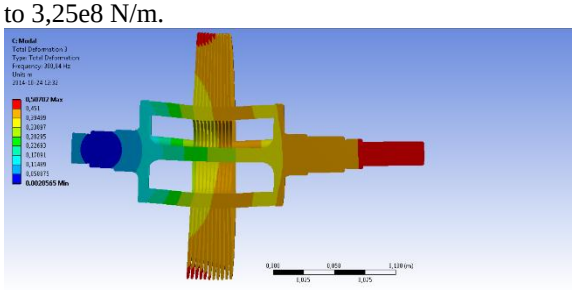

Fig. 21. A mode shape, which can occur in the event of drop in angular bearing stiffness

If, by reason of incorrect reassembly or wear and tear this value drops to around 1.6e7 N/m bending mode shape presented on Fig. 21 may occur. The resonance frequency of vibration for tested rotor is equal to 300 Hz. At that speed the rotor cannot function. This should be born in mind during turbine exploitation and its assembly processes.

5. REFERENCES

[1] Tesla N. *Turbine. Ptent No: 1,061,206,* United States Patent Office of New York, 6 May 1913.
[2] Rice W. Tesla Turbomachinery. *Conference Proceedings of the 4th International Tesla Symposium, Serbian Academy of Sciences and Arts.* September 22-25, 1991, strony 117-125.
[3] Hicks, Keneth. *Method of and apparatus for a multistage bounadry layer engine and process cell. Patent No: 6,973,792 B2* United States Patent Office, 13 December, 2005.
[4] Jędrzejewski Ł., Lampart P. Investigations of aerodynamics of tesla Bladeless microturbines. *Journal Of Theoretical And Applied Mechanics.* No 49, 2, pp. 477-499, Warsaw 2011.
[5] Krzemiński-Freda H. *Łożyska toczne.* wyd. II zmienione. Warsaw : PWN, 1989.
[6] NSK. *Super Precision Bearings - Łożyska Superprecyzyjne.*

Paweł BAGIŃSKI, MSc Eng. – works as an assistant at the Institute of Fluid-Flow Machinery, Gdańsk. His main research interests generally include dynamics of rotating machines supported by gas bearings (mainly foil bearings), slide bearings and rolling bearings.

Łukasz JĘDRZEJEWSKI, MSc Eng. - works as an assistant at the Institute of Fluid-Flow Machinery, Gdańsk. His main research interests generally include: hydrodynamic layer properties on a flat surface under the action of an electrostatic field, micro-stream and biphasic (liquid-liquid or gas-liquid) stream cooling (Gdańsk University of Technology), numerical analysis of range of Tesla turbine models, flow analysis of governing stage in a steam turbine.